Received: 19 November 2017 | Revised: 1 February 2018 | Accepted: 7 March 2018 | Published on: 6 April 2018
DOI: 10.1002/joc.5531

International Journal of Climatology RMetS

RESEARCH ARTICLE

Statistical downscaling of daily precipitation and temperatures in southern La Plata Basin

María Laura Bettolli[1,2] | Olga Clorinda Penalba[1,2]

[1]Departamento de Ciencias de la Atmósfera y los Océanos, Universidad de Buenos Aires, Buenos Aires, Argentina

[2]Consejo Nacional de Investigaciones Científicas y Tecnológicas (CONICET), Buenos Aires, Argentina

Correspondence
María Laura Bettolli, Facultad de Ciencias Exactas y Naturales, Universidad de Buenos Aires, Intendente Güiraldes 2160, Ciudad Universitaria, C1428EGA Buenos Aires, Argentina.
Email: bettolli@at.fcen.uba.ar

Funding information
UBA, Grant/Award Number: 20020130200142BA, 20020130100263BA; CONICET, Grant/Award Number: PIP 0137

La Plata Basin has a considerable socio-economic value, being one of the most important agricultural and hydropower-producing regions in the world. In this region, there is increasing evidence of a changing climate with more frequent and more intense extreme events. Despite the importance of empirical statistical downscaling for regional climate impact studies, few studies have addressed this issue for southern South American regions. In this work, the analogue method was calibrated and validated for simulating local daily precipitation and maximum and minimum temperatures in southern La Plata Basin. The model was trained for the 1979–2000 period and validated for the independent period 2001–2014. Daily fields from NCEP-NCAR Reanalysis 2 were used as predictors and daily observed data from 25 meteorological stations were used as predictands. A variety of potential predictors (including circulation, temperature and humidity variables) and combinations of them over different domain sizes were tested, revealing that the method was more skilful when combined predictors were considered. However, depending on the local predictand and the season of the year different predictor sets may be more appropriate. The method was comprehensively evaluated by means of several skill measures concerning different properties such as mean values, day-to-day variance, daily correspondence, persistence, inter-annual variability, probability distributions and extreme percentiles. The method showed an overall good performance. It tended to overestimate (underestimate) temperature values, especially during winter (summer); however, the day-to-day variance during these seasons was fairly well represented. The method was able to reproduce extreme percentiles and their spatial distributions for the three predictand variables as well as the probability of compound temperature and precipitation extreme events. The performance of the method was very good at estimating seasonal cycles of the different aspects explored. It showed some difficulties in representing the persistence in daily temperatures and the inter-annual variability of seasonal precipitation.

KEYWORDS
analogue method, daily maximum and minimum temperatures, daily precipitation, regional climate, southern South America, statistical downscaling

1 | INTRODUCTION

Located in the southern tip of South America, Argentina has a great variety of climates, mainly given its vast latitudinal extent, its complex orography, its proximity to the Atlantic and Pacific oceans and the influence of the Amazon rain forest (Barros *et al.,* 2006). These features in complex combination with remote forcings contribute to define the climates of Argentina and their variability. With such a varied range of climate regions and in the context of climate change, it is then essential to develop tools to study the regional climate and its possible evolution.

Global climate models (GCM) have been designed to describe large-scale climate characteristics and the potential evolution of climate under future emission scenarios (Meehl *et al.,* 2007). However, GCM still show major deficiencies when it comes to representing small-scale processes that may condition the regional climate (Silvestri and Vera, 2008; Bettolli and Penalba, 2014; Maenza *et al.,* 2017). Therefore, in order to generate climate information at a regional or local scale, it is necessary to apply downscaling techniques to relate large-scale information provided by GCM to the regional-scale climate information needed to assess impacts and decision-making. To obtain high-resolution projections, two approaches are commonly used. Dynamical downscaling techniques are based on regional climate models (RCMs) that simulate regional climate processes with a greater spatial resolution, using GCM fields as boundary conditions (Giorgi and Mearns, 1991; Rummukainen, 2010). On the other hand, empirical statistical downscaling (ESD) methods generate climate information at local scale or with a greater resolution than that achieved by GCMs by means of empirical/statistical relationships between large-scale atmospheric variables and local climate (Hewitson and Crane, 1996; Wilby *et al.,* 2004). Comparative studies between RCM and ESD simulations suggest that both approaches show comparable skills to represent regional climate characteristics (Haylock *et al.,* 2006; Menéndez *et al.,* 2009; Huth *et al.,* 2015), adding value to GCM simulations. Therefore, efforts to develop and validate different regional climate modelling techniques are of great importance not only to better understand the climate system, but also to generate detailed and tailored climate information.

ESD methods have been widely validated and compared for local climate modelling in different regions across the globe (Schoof and Pryor, 2001; Timbal and McAvaney, 2001; Gutiérrez *et al.,* 2005; Hewitson and Crane, 2006; Benestad, 2010; Frost *et al.,* 2011; Gutiérrez *et al.,* 2013, among others) identifying their strengths and weaknesses in each case. Different international initiatives have also contributed to the intercomparison of methods, such as the STARDEX project (Statistical and Regional dynamical Downscaling of Extremes for European regions) (Goodess, 2005), VALUE: COST Action (Validating and Integrating Downscaling Methods for Climate Change Research) (Maraun *et al.,* 2015) and CORDEX-ESD, an initiative by the World Climate Research Programme designed to guide coordinated statistical downscaling experiments and to contribute to the generation and interpretation of region-specific climate change projections (http://cordex.org/domains/cordex-esd/).

In spite of this, in the south of South America the ESD potential to simulate regional climate characteristics has not been explored as thoroughly or systematically as in other parts of the world. With regard to previous applications of statistical downscaling methods in Argentina, Solman and Núñez (1999) adjusted the stepwise multiple linear regression technique to downscale monthly mean values of surface air temperature (maximum, minimum and mean temperatures) and estimate their future local changes in the central eastern region of Argentina. The same technique was used by Labraga (2010) to statistically downscale monthly precipitation values in three regions of the Argentine Andes. At a daily scale, Cavazos and Hewitson (2005) evaluated the relative efficiency of several atmospheric predictors of daily precipitation in different locations worldwide, one of them located in the Argentine Pampas, using artificial neural networks and rotated principal component analysis. D'onofrio *et al*. (2010) assessed the *k*-means technique and the self-organizing maps (SOM) for probabilistic estimates of daily rainfall in different regions of Argentina. Bettolli *et al*. (2010a) used the SDSM model (Wilby *et al.,* 2002) to analyse the possible implications of future climate change for natural pasture yield in Salto, a district on the border between Argentina and Uruguay. Probabilistic estimates of daily rainfall and daily maximum and minimum temperatures in central northeastern Argentina were also assessed by means of different clustering methods such as *k*-means (Penalba *et al.,* 2013; Bettolli and Penalba, 2014) or SOM (Espinoza *et al.,* 2012). Furthermore, in order to contribute to the intercomparison effort of ESD methodologies within the CORDEX framework, the first coordinated experiment of CORDEX-ESD was conducted in the La Plata Basin (http://www.cordex.org/experiment-guidelines/cordex-esd-protocol.html), the results of which are being analysed.

All that has been mentioned so far evidences the need to move forwards with studies on the ESD methods performance to simulate the regional climate of the different regions across Argentina. There is a variety of ESD methods that can be explored. These methods can be classified according to different criteria, depending on their approach, implementation and application (Wilby and Wigley, 1997; Wilby *et al.,* 2004; Maraun *et al.,* 2010). In general terms, ESD methods can be categorized into subgroups which include transfer functions (linear or nonlinear), weather generators and weather typing methods and analogues. In the latter, the downscaling methods relate weather classes to local and regional weather conditions. In particular, in the analogue method, historical large-scale weather situations similar (according to a selected metric) to the large-scale weather situation on a given target day are identified. Then, the corresponding historical local weather conditions are used to estimate local weather conditions on the target day (Zorita and von Storch, 1999). This method has been used, either in its classic version or in more sophisticated ones, in many regions with different physiographic characteristics showing good performances at estimating local conditions. With a relatively simple design, it has

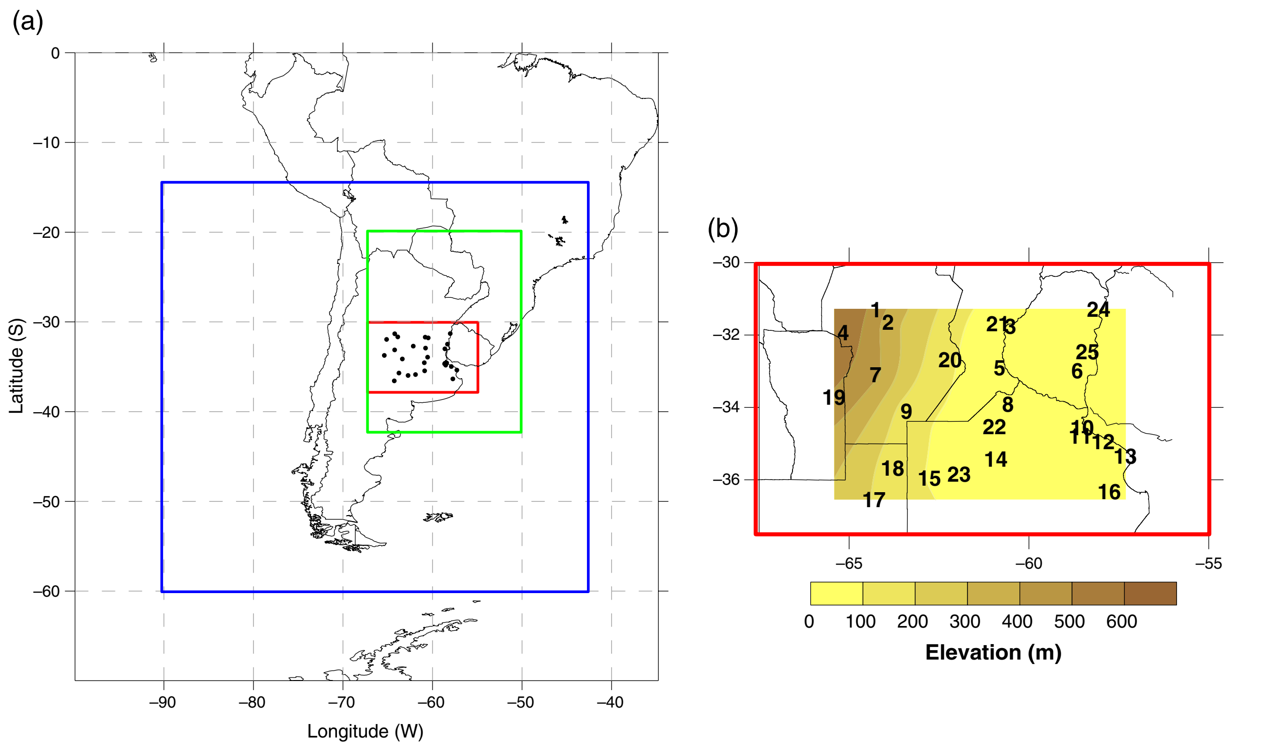

FIGURE 1 Area of study. (a) Domains of the predictor variables tested: LD (blue), MD (green) and SD (red). (b) Location of the meteorological stations used, see Table 1 for specifications [Colour figure can be viewed at wileyonlinelibrary.com]

shown to perform as well as more complicated methods (Zorita and von Storch, 1999; Schmidli *et al.*, 2007; Frost *et al.*, 2011; Gaitan *et al.*, 2014; Maraun *et al.*, 2017), being able to be applied to both normally and non-normally variables such as local temperatures and precipitation (Timbal and McAvaney, 2001; Timbal *et al.*, 2003; Imbert and Benestad, 2005; Timbal and Jones, 2008; Benestad, 2010; Brands *et al.*, 2011; Ribalaygua *et al.*, 2013, among others). Therefore, the objective of this study is to calibrate and validate the analogue method as a technique to downscale daily precipitation and maximum and minimum temperatures in southern La Plata Basin (Figure 1). This region in particular was selected mainly because it extends over the most productive agricultural area in the country (the Pampas region), whose predominant activities are extensive rainfed agriculture and livestock farming. Furthermore, it is in this area where large cities are located, such as Buenos Aires and its metropolitan area, home to more than 12 million inhabitants (INDEC, 2010)—concentrating the highest population density in Argentina.

2 | DATA AND METHODOLOGY

2.1 | Data

Daily precipitation (Pr), maximum and minimum temperatures (Tx and Tn, respectively) from 25 meteorological stations were used as predictand variables (Table 1). These stations, located in the southern La Plata Basin region (Figure 1), were provided by the National Weather Service of Argentina and have less than 10% of missing data (Table 1).

Daily fields from NCEP Reanalyses II (Kanamitsu *et al.*, 2002) were used as large-scale predictor variables. Regional circulation in South America is strongly influenced by the Andes range. Between 10°S and 40°S, the mountains completely block the westerly flow in the lower troposphere and tend to strongly channel the meridional flow (Seluchi and Marengo, 2000). Meridional transport of air masses in both senses between the tropics and mid-latitudes is then intense in the eastern side of the Andes. North of 40°S, cooling is the consequence of northwards intrusions of cold fronts and, therefore, warming in this region predominates when the frontal zone remains at higher latitudes (Barros *et al.*, 2002a). Taking into account these regional circulation characteristics, a basic correlation screening analysis and previous studies based on weather typing schemes (Espinoza *et al.*, 2012; Penalba *et al.*, 2013; Bettolli and Penalba, 2014), three different spatial domains were considered depending on the large-scale variable (Figure 1). The large domain (LD) covers part of the Pacific and Atlantic oceans and the Andes range, affecting the circulation structure and the systems configuration. On the other hand, the middle (MD) and small (SD) domains encompass regions to the east of the Andes, concentrating the regional processes that control temperature and humidity

TABLE 1 Meteorological stations used in the study (MD = missing data)

Code	Name	WMO code	Latitude (°S)	Longitude (°W)	Elevation (m)	MD Tn (%)	MD Tx (%)	MD Pr (%)
1	Córdoba Aero	87344	−31.32	−64.22	474	1.57	1.86	0.46
2	Pilar Observatorio	87349	−31.67	−63.88	338	0.08	0.43	0.00
3	Paraná Aero	87374	−31.78	−60.48	78	0.19	0.14	0.03
4	Villa Dolores Aero	87328	−31.95	−65.13	569	0.21	0.13	0.11
5	Rosario Aero	87480	−32.92	−60.78	25	0.06	1.32	0.00
6	Gualeguaychú Aero	87497	−33	−58.62	21	0.07	0.07	0.00
7	Rio Cuarto Aero	87453	−33.12	−64.23	421	0.52	1.54	0.26
8	Pergamino INTA	87484	−33.93	−60.55	65	7.34	7.22	6.20
9	Laboulaye Aero	87534	−34.13	−63.37	137	0.02	0.23	0.00
10	Buenos Aires OCBA	87585	−34.58	−58.48	25	0.02	0.24	0.00
11	Ezeiza Aero	87576	−34.82	−58.53	20	0.37	0.36	0.00
12	La Plata Aero	87593	−34.97	−57.9	19	2.33	3.27	0.28
13	Punta Indio Aero	87596	−35.37	−57.28	22	1.87	1.71	1.60
14	9 de Julio	87550	−35.45	−60.88	76	0.82	0.84	0.63
15	Trenque Lauquen	87540	−35.97	−62.73	95	8.10	8.13	8.21
16	Dolores Aero	87648	−36.35	−57.73	9	8.91	5.29	2.28
17	Santa Rosa Aero	87623	−36.57	−64.27	191	0.02	0.00	0.00
18	General Pico Aero	87532	−35.70	−63.75	145	0.20	0.66	0.00
19	Villa Reynolds Aero	87448	−33.73	−65.38	486	0.17	0.08	0.02
20	Marcos Juárez Aero	87467	−32.70	−62.15	114	2.17	2.97	0.02
21	Sauce Viejo Aero	87371	−31.70	−60.82	18	0.41	0.34	0.26
22	Junín Aero	87548	−34.55	−60.92	81	0.05	0.04	0.00
23	Pehuajó Aero	87544	−35.87	−61.90	87	2.09	1.33	0.03
24	Concordia Aero	87395	−31.3	−58.02	38	0.05	0.28	0.00
25	Concepción del Uruguay	87494	−32.48	−58.33	25	9.79	9.69	9.74

advections. It is worth noting here that although the three domains analysed encompass much of the predictor–predictand relationships, some South American regional features and remote forcings, which are not directly contained within the chosen domains, may have strong relationships with local conditions such as the South American low-level jet, the South American monsoon or the South Atlantic convergence zone (Barros *et al.,* 2002b).

A variety of potential predictors and combinations of them were tested. They include upper-air circulation, temperature and humidity variables: geopotential height at 500 (Z500) and 200 (Z200) hPa, meridional and zonal wind components at 850 hPa (V850 and U850, respectively), mean sea level pressure (SLP), air temperature at 850 hPa (T850), relative and specific humidity at 850 hPa (RH850 and Q850, respectively). The predictor variables in each domain will be indicated as follows: variable_domain, for example, SLP_MD indicates the variable mean SLP in the medium domain.

Direct surface variables (Tx, Tn and Pr) from the reanalysis were also considered for comparisons with station data.

The period of analysis was 1979–2014, which was conditioned by the start of the reanalysis data and the end of the observational data available at the time of the study.

2.2 | Methods

The analogue technique (AN) was used in its classic version (Zorita and von Storch, 1999). The empirical orthogonal functions (EOF) technique was used in order to reduce the dimensions of predictor variables. Previously, the temporal series of predictor variables in each grid point were standardized and then geographically balanced by the cosine of the corresponding latitude (Benestad *et al.,* 2008; Brands *et al.,* 2011). In each case, the principal components that accounted for at least 99% of the variance were retained.

The analogue method consists of finding, for each day in the record, the most similar large-scale situation (the nearest neighbour). The similarity was assessed using the Euclidean distance. In this work, the analogue model was trained for the 1979–2000 period and then it was applied to the independent period 2001–2014. The analogue search was unrestricted, that is, the analogues were not restricted to the season of the year of the target day (Imbert and Benestad, 2005). For the training process, an analogue for a target day was searched for over all of the days excluding the 183 days preceding and the 183 days following the target day. That is, a moving window of 367 days centred in the target day to avoid artificial skills due to persistence or intra-annual relationships, for instance, those associated with the El Niño-Southern Oscillation (ENSO) phenomenon. This forcing has a strong effect in inducing circulation anomalies over the region which are manifested in changes in weather type frequencies and their related local conditions as shown by Bettolli, Penalba, and Vargas (2010b). In this process different potential predictor variables and combinations of up to 4 of them were explored. The final selection of suitable predictors was based on the evaluation of daily root-mean-square errors (RMSE) and the index *I*, which measures the skill of the AN method in reproducing wet days (Timbal *et al.,* 2003), defined as follows:

$$I = 100 \times \left(1 - \frac{m}{w+m} - \frac{f}{d+f}\right),$$

where w is the number of observed and downscaled wet days, d is the number of observed and downscaled dry days, m is the number of observed wet days and missed by the AN and f is the number of observed dry days and missed by the AN. A wet day is considered a day with Pr > 0.1 mm/day. The index can vary from 0 (no skill) to 100 (perfect scheme).

Different metrics can be considered to evaluate the performance of an ESD method depending on the application of interest. These take into account the different aspects of the system, such as marginal, temporal, spatial and inter-variable aspects (Maraun *et al.,* 2015). In this work, a suite of validation measures was considered in order to perform a comprehensive assessment of the method performance. The mean difference between simulated and observed daily values (BIAS) was assessed for temperatures. Mean daily precipitation intensity (wet day intensity) and the probability of a wet day (wet day occurrence) were compared with observations through the ratio between downscaled and observed values, as well as the day-to-day variance of Tn, Tx and Pr. The daily correspondence was quantified using the nonparametric Spearman correlation to minimize artificial skills due to the not normally distributed temperatures and precipitation. Also, the Pearson correlation coefficient for seasonal aggregated values was used as an indicator of the methods' ability to capture inter-annual variations. The day-to-day persistence was assessed considering the auto-correlations lagged by 1 day for temperatures and the conditional probabilities of having a wet day if the previous day was wet (wet–wet) and of having a wet day if the previous one was dry (dry–wet).

The statistical distributions of downscaled Tx, Tn and Pr were compared to the corresponding observed distributions using the two-sample Kolmogorov–Smirnov (K–S) test with a confidence level of 95% (Wilks, 2006). For daily precipitation, the distributions of wet days were considered, defined as those with a Pr higher than 0.1 mm/day. The 75th and 95th percentiles of wet days were validated, corresponding to extremes relevant in various impact sectors in the region (Robledo *et al.,* 2013). For temperatures, the skewness and the 5th and 95th percentiles of the probability distributions were also compared.

To evaluate the inter-variable relationships, compound extreme events of precipitation and temperature were tested according to the definition given by Tencer *et al*. (2016). The authors found that events of intense precipitation during days with high minimum temperature are the most significant in the region. Therefore, in this study compound extreme events, defined as the combined occurrence of heavy precipitation events identified as those days when the daily precipitation exceeded the 75th percentile of the empirical distribution of wet days (Pr75) and extreme temperature events considered as those days when Tn exceeded the 90th percentile (Tn90) of the empirical distribution of all days in a season, were analysed. The authors also found that the probability of occurrence of intense precipitation events significantly decreases during days with low temperature (minimum temperature lower than the 10th percentile-Tn10). The conditional probability of Pr75 given Tn10 was additionally evaluated. The conditional probability of the heavy precipitation event given the occurrence of an extreme Tn event was expressed as a ratio over the expected probability in the absence of a relationship, that is, the probability of occurrence of a day with precipitation above the 75th percentile itself. Ratios between 0 and 1 will depict a negative relation between the extremes, and, therefore, a lower probability of heavy precipitation given that temperatures are extreme. Ratios greater than 1 describe a positive relation between extreme temperature and precipitation events, with the probability of heavy precipitation being increased by the occurrence of a temperature extreme.

The analysis was conducted on an annual basis and for the four austral seasons: summer (DJF), fall (MAM), winter (JJA) and spring (SON).

3 | RESULTS

3.1 | Predictor selection

An important aspect in the statistical downscaling process is the selection of suitable predictors. These will depend not only on the region and the season considered but also on the predictand variable (Huth, 1999; 2004; Cavazos and Hewitson, 2005; Labraga, 2010). Furthermore, for climate change applications, predictors must be realistically reproduced by GCMs and the relationship between predictors and predictands needs to be stationary (Maraun *et al.,* 2010).

In order to select informative predictors for the statistical downscaling of daily maximum and minimum temperatures and precipitation, different large-scale variables (single predictors), together with their combinations (combined predictors) were considered in different domains. Figure 2 shows the boxplots of daily RMSE of the downscaled values

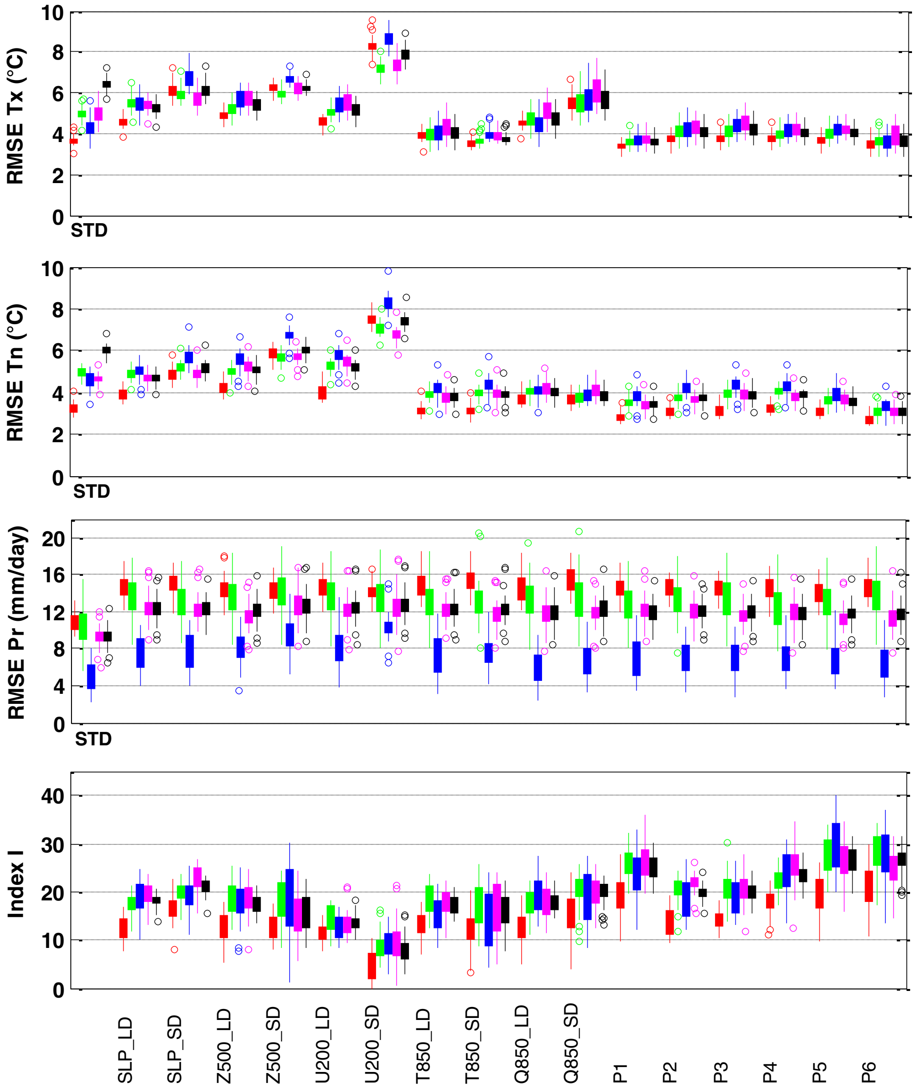

FIGURE 2 Box and whisker plots of daily RMSE across all stations for Tx (first panel), Tn (second row) and Pr (third row), and of index *I* (fourth row) for selected single predictor and predictor combinations. Each group of five boxplots corresponds to each single predictor or predictor combinations for summer (red), fall (green), winter (blue), spring (pink) and annual (black) errors. On each box, the central mark indicates the median, and the bottom and top edges of the box indicate the 25th and 75th percentiles, respectively. The whiskers extend to the most extreme data points not considered outliers, and the outliers are plotted individually using the "o" symbol. STD corresponds to the observed daily *SD*. Because of space shortage P1 = SLP_MD_T850_SD; P2 = SLP_LD_T850_MD, P3 = Z500_LD_T850_MD, P4 = U850_V850_MD_T850_SD, P5 = U850_V850_MD_T850_RH850_SD and P6 = SLP_MD_T850_Q850_SD [Colour figure can be viewed at wileyonlinelibrary.com]

relative to the observed values across all stations. Although different combinations of variables and domains were analysed, for brevity, this figure only shows some representative cases of the general results. For each single predictor variable or combination of predictor variables, the summer, fall, winter, spring and annual RMSE distribution is shown. In order to make a comparison with a reference value, the boxplot of the observed daily standard deviations (*SD*) was added.

For Tx and Tn, RMSE are high when considering only the circulation variables as predictors (SLP, Z500 and U200), surpassing the observed daily *SD*. In this case, it can be seen that as the domain size decreases, errors increase, showing the importance of capturing the large-scale circulation structures that control the regional temperatures. In both predictand variables, accuracy is enhanced if the thermal information given by T850 is considered, whereas the specific humidity at 850 hPa (Q850) shows a better skill to downscale local daily minimum temperature. When the different combinations of predictors and domains (P1–P6 predictors) are considered, the RMSE in temperatures decrease, especially for Tn in line with the findings by other authors (Timbal *et al.,* 2003; Huth, 2004; Brands *et al.,* 2011). The seasonal variation of errors shows that the lowest errors in Tn and Tx generally occur in summer (red boxplots), except for some cases as in single predictors Z500_SD, U200_SD and Q850_SD. When compared with the observed daily *SD* in temperatures, it is possible to see that it is minimum in summer—a characteristic that the AN method captures correctly, taking into account that the search of analogues was unrestricted. For Tn, the major errors occur in winter (blue boxplots) for all the potential predictor sets studied except when the specific humidity is considered in the smallest domain as a single predictor. This is probably due to the fact that minimum temperatures are mainly affected by local conditions, specially the coldest ones, and the unrestricted search of the analogues may not be able to capture this feature. For Tx, on the other hand, the greater errors are observed mainly in winter if single predictors of circulation are considered, while they are more evident in spring (pink boxplots), when temperature and humidity are considered as either single predictor or combined predictors. The lower dispersions in RMSE (smaller boxes) are also observed in Tn in all seasons of the year, when compared to Tx.

For daily precipitation values, errors are relatively high for all the predictor sets analysed (single predictors or combined predictors). However, when the occurrence of precipitation is evaluated through index *I* (Figure 2, fourth row) the method is more skilful when combined predictors are considered, in particular in the case of the combinations that consider humidity variables within their predictors (P5 and P6). The RMSE of precipitation in winter are the lowest (blue boxplots), coinciding with the lower values of the *SD* observed, while the performance of the method is reduced in summer. This is probably because winter precipitation is mostly controlled by large-scale mechanisms that are well captured by the AN. When analysing the occurrence of wet and dry days through index *I*, it is possible to observe that the method shows a lower performance again in summer, while its performance in the other seasons of the year depends on the predictor set (for instance, for the P1 combination, the best skill of the model in Index I occurs during spring).

As shown in the previous analysis, depending on the local predictand and the season of the year different predictor sets may be more appropriate. However, in order to ensure the physical consistency of the local values estimated with the analogue method, for this study it was decided to use the same predictor set for the three variables (Tx, Tn and Pr) which corresponds to the combination P6: SLP_MD, T850_SD and Q850_SD, showing low relative RMSE values and high values of the index *I*.

3.2 | Validation

Once the predictor set has been selected, the AN method was applied to the independent period 2001–2014. Metrics for comparisons between downscaled and observed values of Tx, Tn, Pr occurrence and Pr amount are shown in Figure 3.The figure shows the daily BIAS and variance expressed as a ratio over the observed value for Tx and Tn jointly with the wet day occurrence, wet day intensity and variance expressed as a ratio over the observed value for Pr. The daily correspondence between downscaled and observed values measured by the Spearman correlation coefficient is also displayed. In order to explore the added value of the statistical method, these metrics were compared with the direct daily outputs from the reanalysis. The comparison with the observations at station point considered the closest grid point. Although this procedure has limitations, because the values at grid point represent mean areal values, it was taken as a reference point.

For maximum and minimum temperatures (Figure 3a), the AN tends to overestimate the temperatures values in winter (areal average of 0.71 and 0.76 °C for Tx and Tn, respectively) and to underestimate them in spring (areal average of −0.99 and −0.51 °C for Tx and Tn, respectively). The summer minimum temperatures are also underestimated by the AN method although with average areal values of −0.62 °C. The AN method outperforms the raw reanalysis outputs, being more evident for Tn, which shows areal average biases that surpass 1.5 °C in all seasons. For both temperatures, the analogue method tends to overestimate the day-to-day variance, particularly during the transition seasons. However, the AN method improves notably the reproduction of the variance when compared to the direct reanalysis data. As to the temporal correspondence measured by daily correlation, in both temperatures the highest values are shown by the reanalysis. The AN method is not able to correctly represent the temporal correspondence especially during summer and winter. The Pearson correlation was also calculated for Tx and Tn (not shown) and similar results were found.

The wet day intensity is fairly well represented by the analogue method (Figure 3b). The observed mean daily intensity across the region varies from 7.15 mm/day in winter to 14.56 mm/day in summer, taking values of about 12 mm/day in the transition seasons. This seasonal variation is very well captured by the method. Instead, the wet day occurrence tends to be overestimated during winter and underestimated in spring, with high spread across stations. Even so, AN outperforms NCEP raw data, which shows less frequent and more intense daily precipitation than observed. Daily correlations for NCEP are slightly higher than AN, but they remain low. Although not shown, the day-to-day variance was also evaluated for precipitation, revealing that the AN method tends to overestimate (underestimate) it during winter with areal averages of 1.23 (0.83) relative to the observed variance. Meanwhile, NCEP raw precipitation underestimates variance in all seasons of the year being poorest during summer and fall (areal averages of 0.58 and 0.56, respectively).

The temporal structure quantified by the autocorrelations lagged by 1 day for temperatures and the wet–wet and dry–wet transition probabilities for precipitation are shown in Figure 4. The persistence of both temperatures is generally underestimated by the AN method, in particular during summer and winter. In turn, the autocorrelation values in transition seasons and throughout the year are better represented. The wet–wet conditional probabilities are very well captured in summer and slightly underestimated in fall, spring and on an annual basis. On the other hand, in winter there is a greater underestimation, with a high dispersion of values across stations. The dry–wet transition probabilities are quite well represented by the method, whereas being slightly overestimated in transition seasons.

The inter-annual correspondence between downscaled and observed seasonal values was evaluated through the Pearson correlation coefficient and its spatial distribution is presented in Figure 5 for the period 2001–2014. The downscaling model tends to have better skill for Tn, for all the seasons of the year although Figure 5 only shows winter and summer. In winter agreement is very high, when 23 of

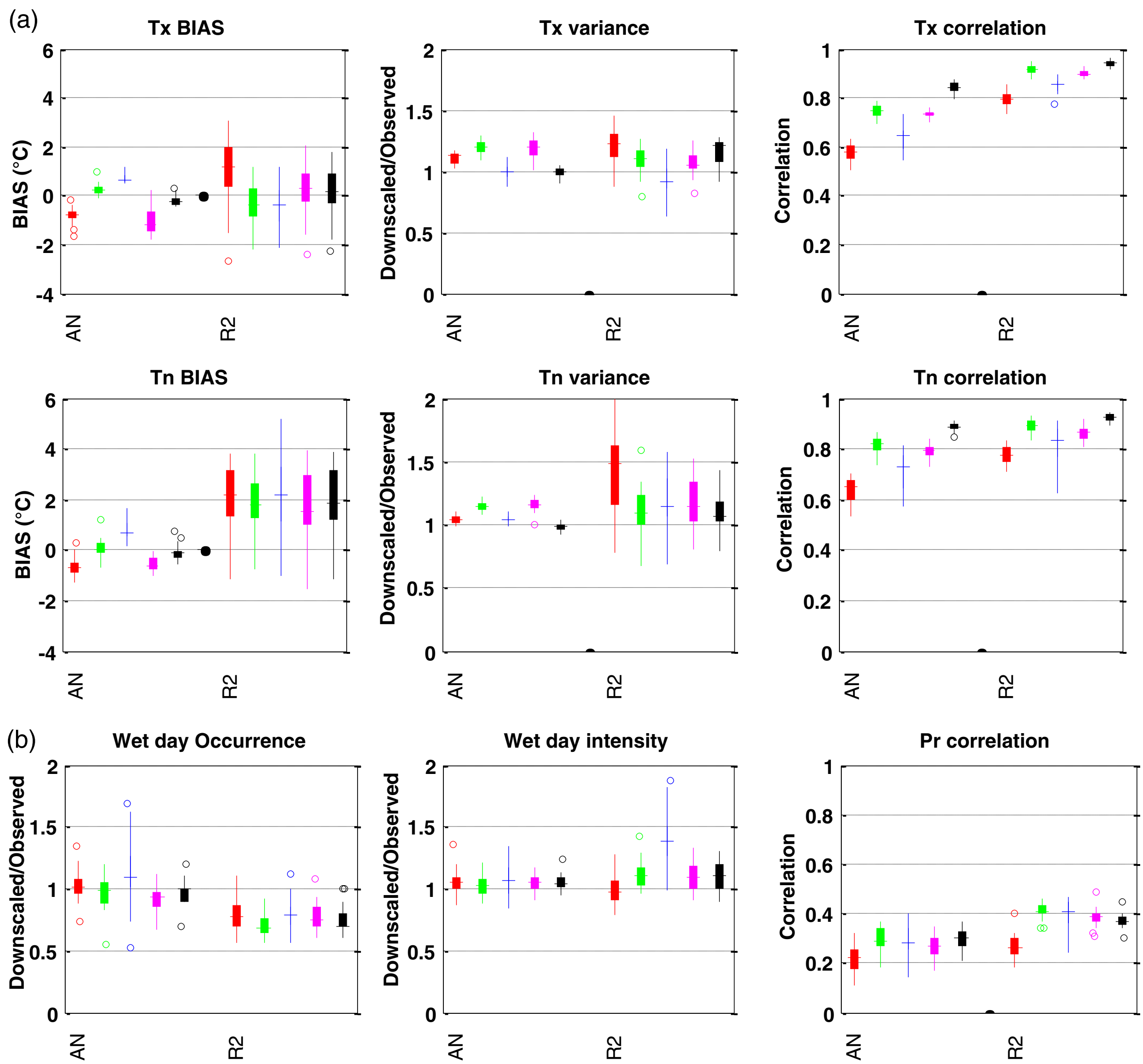

FIGURE 3 (a) Box and whisker plots of daily BIAS, variance expressed as a ratio over the observed value and Spearman correlation across all stations for Tx and Tn. (b) Box and whisker plots of wet day occurrence and wet day intensity expressed as a ratio over the observed value and Spearman correlation across all stations for Pr. Values for summer (red), fall (green), winter (blue), spring (pink) and annual (black) periods are displayed for the AN and direct output from reanalysis (R2) [Colour figure can be viewed at wileyonlinelibrary.com]

25 stations show correlations above 0.8. For Tx, the intensity of the agreement is slightly lower although it keeps being satisfactory, especially for winter. For the seasonal precipitation amounts, correlations weaken in both seasons of the year, showing higher values in the stations located along the central band of the studied area. The seasonal frequencies of wet days (Fr) show a better agreement during winter and fall (not shown). This is related to the fact that during the cold season, the most relevant precipitation forcing in the region of study is due to synoptic activity, and these large-scale structures can be suitably captured by the AN method. These results are consistent with the findings presented by Timbal (2004) for the western region in France. The lowest performance is observed in stations with a marked dry season in winter. These stations are located towards the inner areas of the continent or in the northwestern zone of the analysed domain, where orographic effects start to have a relevant role as local rainfall forcings (see station altitude in Table 1).

Several authors have documented the rainfall and temperature trends in southeastern South America, overlapped to a large decadal variability (Penalba and Vargas, 2004; Rusticucci, 2012; Maenza *et al.,* 2017). In the eastern margin of the domain analysed, there is a strong consensus concerning the progressive increase up to the present of annual rainfall mainly due to the increases in rainfall during the summer (de Barros Soares *et al.,* 2016; Saurral *et al.,* 2017). Whereas to the southwest, the region underwent a sudden rise in summer precipitation by mid-1970s owing to the influence of the 1976/1977 climate transition (Agosta and Compagnucci, 2012), which caused the shift towards the west of the agricultural barrier of the humid Pampas (border between the humid and semi-arid regions). However, these precipitation trends seem to have reversed after the early

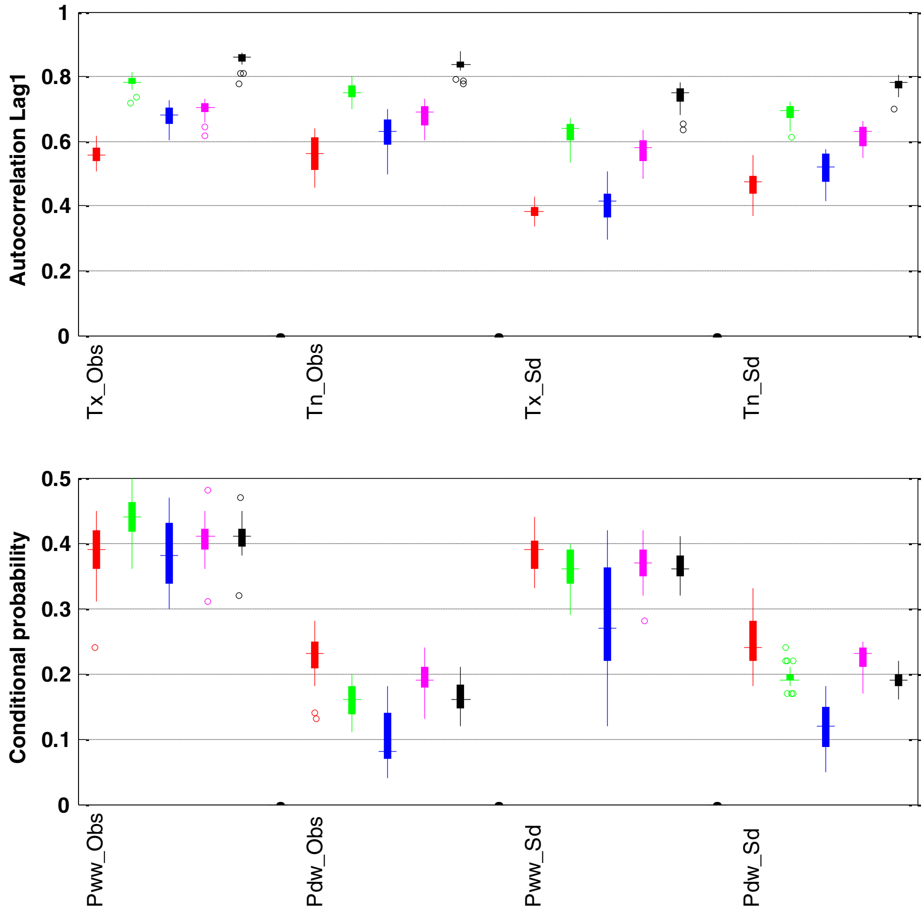

FIGURE 4 Box and whisker plots of observed (Obs) and downscaled (Sd) autocorrelation lagged by 1 day across all stations for Tx and Tn (upper panel) and box and whisker plots of observed and downscaled wet–wet and dry–wet transition probabilities for Pr (bottom panel, note the scale change on *y*-axis), for summer (red), fall (green), winter (blue), spring (pink) and annual (black) periods [Colour figure can be viewed at wileyonlinelibrary.com]

2000s (Maenza *et al.,* 2017). In order to analyse if the recent changes in summer precipitation were reproduced by the AN method, Figure 6 shows the decadal averages of observed and downscaled summer total precipitation for the Buenos Aires station, as representative of the stations located in the east–southeast area of the region studied, and for the General Pico station, as representative of the stations located in the southwestern area. To depict the precipitation evolution in time, the total period is shown (1979–2014), which includes the training period (1979–2000) and the independent period of validation (2001–2014), though the independent period is the focus of our analysis. It should be considered that only 5 years of the 2010 decade are available, but results are shown in order to stress the trend over the recent past years. In the Buenos Aires station, it is possible to observe a progressive growth of summer precipitation mean, with a remarkable increase in the last 5 years, which is in agreement with the findings of Saurral *et al.* (2017). Meanwhile, the change to drier conditions in General Pico station is clearly represented by the analogue method and consistent with the results of Maenza *et al.* (2017).

The results from the K–S test show that the maximum temperature is the variable with the greatest differences in the probability distributions across all the seasons of the year (Figure 7), rejecting the null hypotheses in 23 of 25 meteorological stations during fall and winter. In the case of minimum temperatures, the highest differences can be found during the summer and at an annual scale. For precipitation, there are almost no significant differences between distributions except for 9 of the 25 stations when the full year is considered. The output from the K–S test is the absolute value of the difference between the two cumulative distribution functions, but the test does not provide information about the shape of the distributions. For that reason, the skewness of the observed and downscaled distributions were also evaluated (Figure 8a). Observed Tx and Tn are positively skewed in winter and negatively skewed in summer. During the transition seasons, the skewness tends to zero for Tx but it remains negative for Tn in agreement with the findings of Rusticucci and Barrucand (2001) in a 40-year study. The AN method is able to represent this seasonal variation in the asymmetry of the distributions. The greatest differences are found in summer, especially for Tn.

Figure 8b shows the spatial distribution of the downscaled and observed values and their differences for the 95th percentile of maximum temperature in summer and the 5th percentile of minimum temperature in winter. Although most of the Tx probability distributions show significant differences (Figure 7), the high summer temperatures (95th percentile) are very well represented by the AN method, except for the stations located in the western most continental areas, where the highest 95th Tx percentiles are observed. The stations located in the rest of the region also

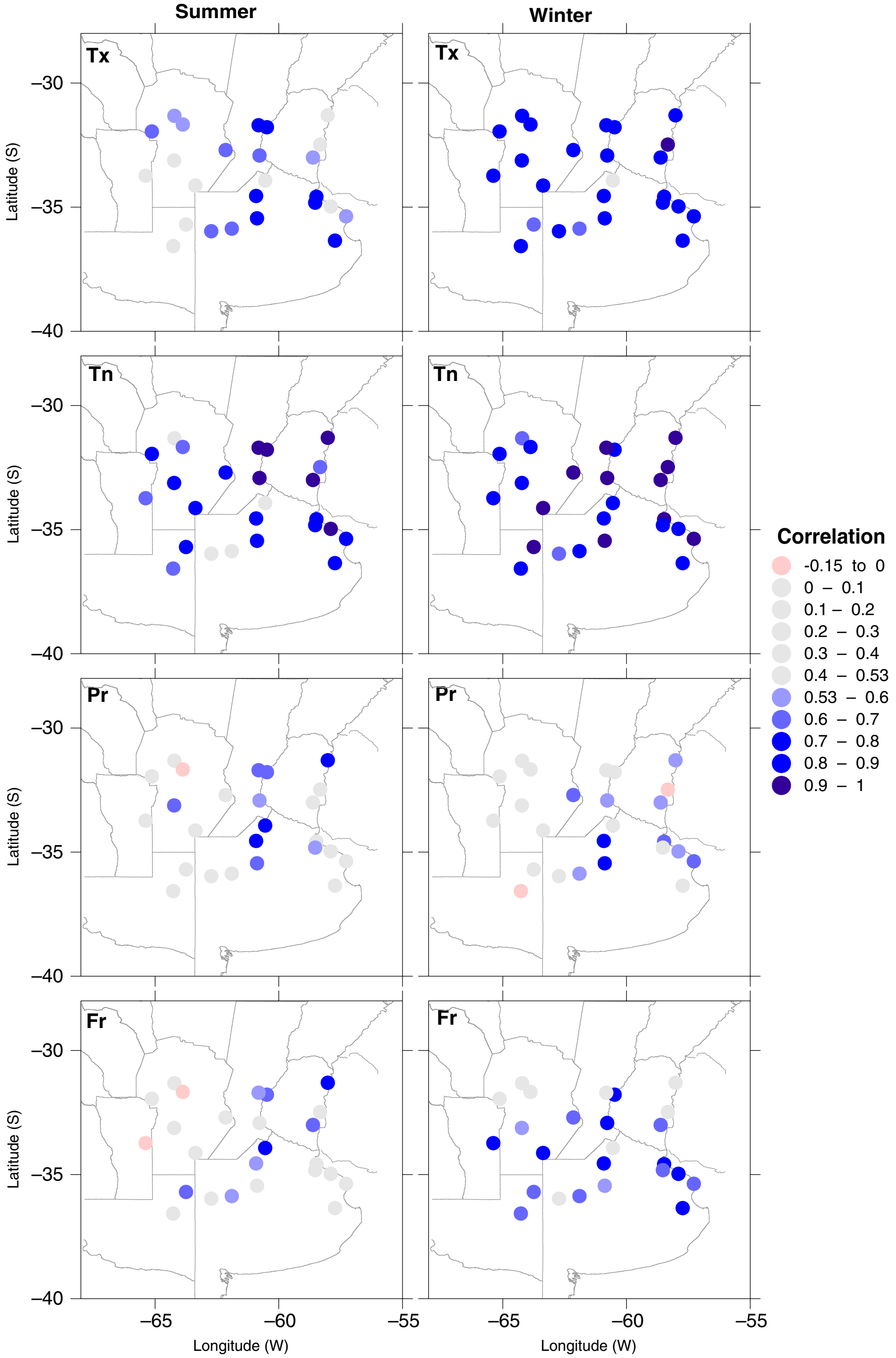

FIGURE 5 Correlations between observed and downscaled seasonal time series for summer and winter. Correlation values greater than 0.53 are significant at the 5% level with a Student's *t* test. Fr: frequency of wet days (Pr > 0.1 mm/day) [Colour figure can be viewed at wileyonlinelibrary.com]

show a very good estimation of high temperature values. Although the 95th percentile tends to be underestimated, except for the stations located in the central north and north-east of the area studied where it is slightly overestimated, the difference of the 95th percentiles does not exceed 1 °C in absolute value. Likewise, the spatial structure of extreme minimum temperatures in winter is very well simulated with a general tendency to be slightly overestimated. The absolute differences in percentiles do not exceed 0.5 °C in 17 of the 25 stations. For precipitation, the analysis of the 75th and 95th percentile shows that the method is able to very accurately represent these extremes throughout all the seasons of the year (Figure 9a). The most accurate representation of spatial distributions of these extreme values is exhibited in spring (Figure 9b) and when the whole year is considered (not shown). During fall some differences become evident, however the gradient of the 95th percentile from the southwest to the northeast is captured (Figure 9b). Similar results are found for summer and winter (not shown).

The accurate representation of extreme values is one of the most important aspects in validating the ESD methods based on its usefulness in impact studies. In this case, it takes on a particular interest because in densely populated

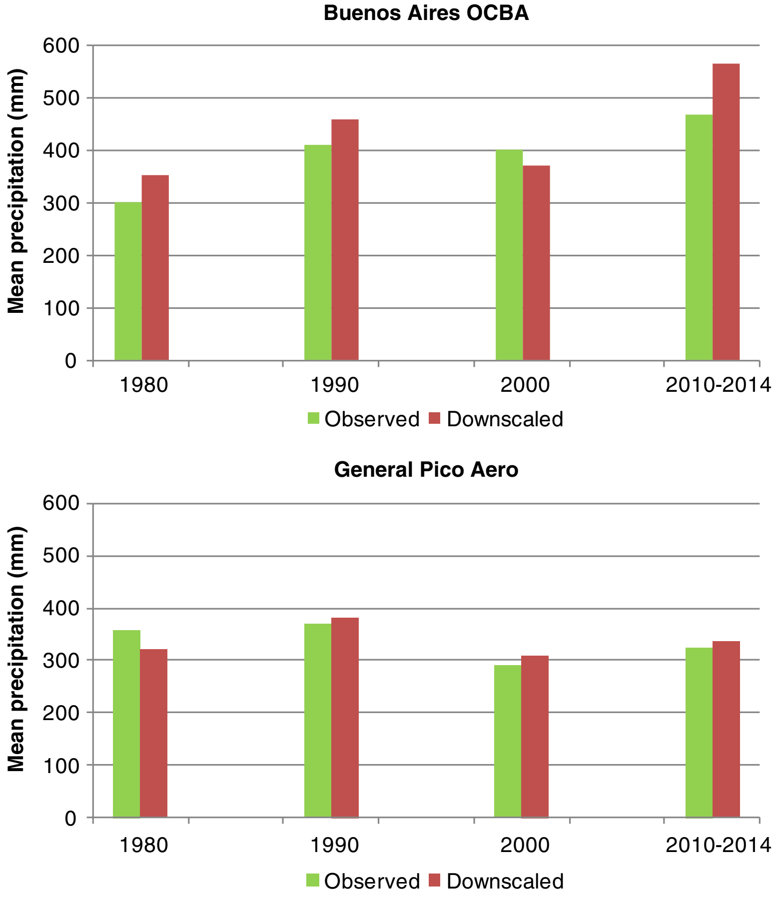

FIGURE 6 Decadal evolution of summer mean precipitation (mm) for the Buenos Aires OCBA station (St. 10) and the General Pico Aero station (St. 18). Note that in the last decade analysed only 5 years are considered in order to depict the recent precipitation trend [Colour figure can be viewed at wileyonlinelibrary.com]

areas (such as the city of Buenos Aires and the Metropolitan area), extreme temperature and precipitation events have a strong impact on the population and result in a great energy demand. Moreover, summer crops (mostly soybean and corn) in the core agricultural region of Argentina are highly affected by thermal stress and water availability. In this context, extreme events were further examined by analysing the joint occurrence of daily extreme temperature and heavy precipitation events. Figure 10 shows the conditional probability of heavy precipitation events (Pr75) given the occurrence of a temperature extreme event (Tn90). Ratios between 0 and 1 will depict a negative relation between the extremes, and therefore lower probability of heavy precipitation given that temperatures are extreme. Ratios greater than 1 describe a positive relation between extreme temperature and precipitation events, with the probability of heavy precipitation being increased by the occurrence of a temperature extreme. In all the seasons of the year, the method can capture the relationship between extremes both in intensity and in spatial distribution. In winter, the conditional probabilities are slightly overestimated in the southwestern area of the region studied. This can be related to the fact that during the cold season the frequency of these compound extremes is relatively low when compared to the other seasons of the year. When calculated separately both the 90th percentile of Tn (not shown) and the 75th percentile of wet days (Figure 9) in winter are very well reproduced. These results indicate that the method is skilful to capture the

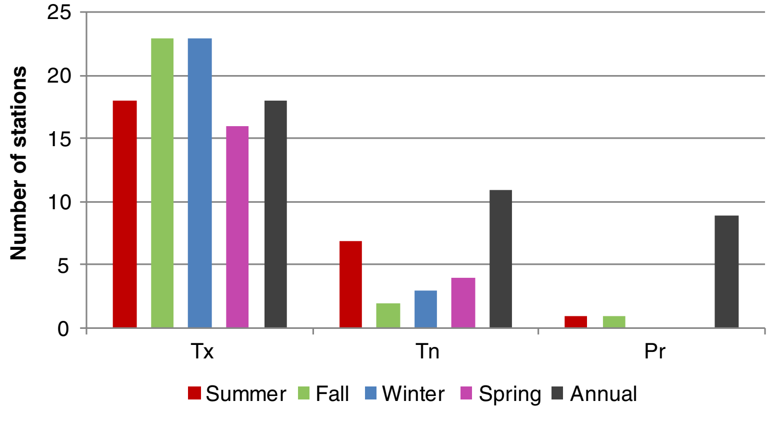

FIGURE 7 K–S test results showed as the number of stations where the probability distributions differed at the 5% significance level [Colour figure can be viewed at wileyonlinelibrary.com]

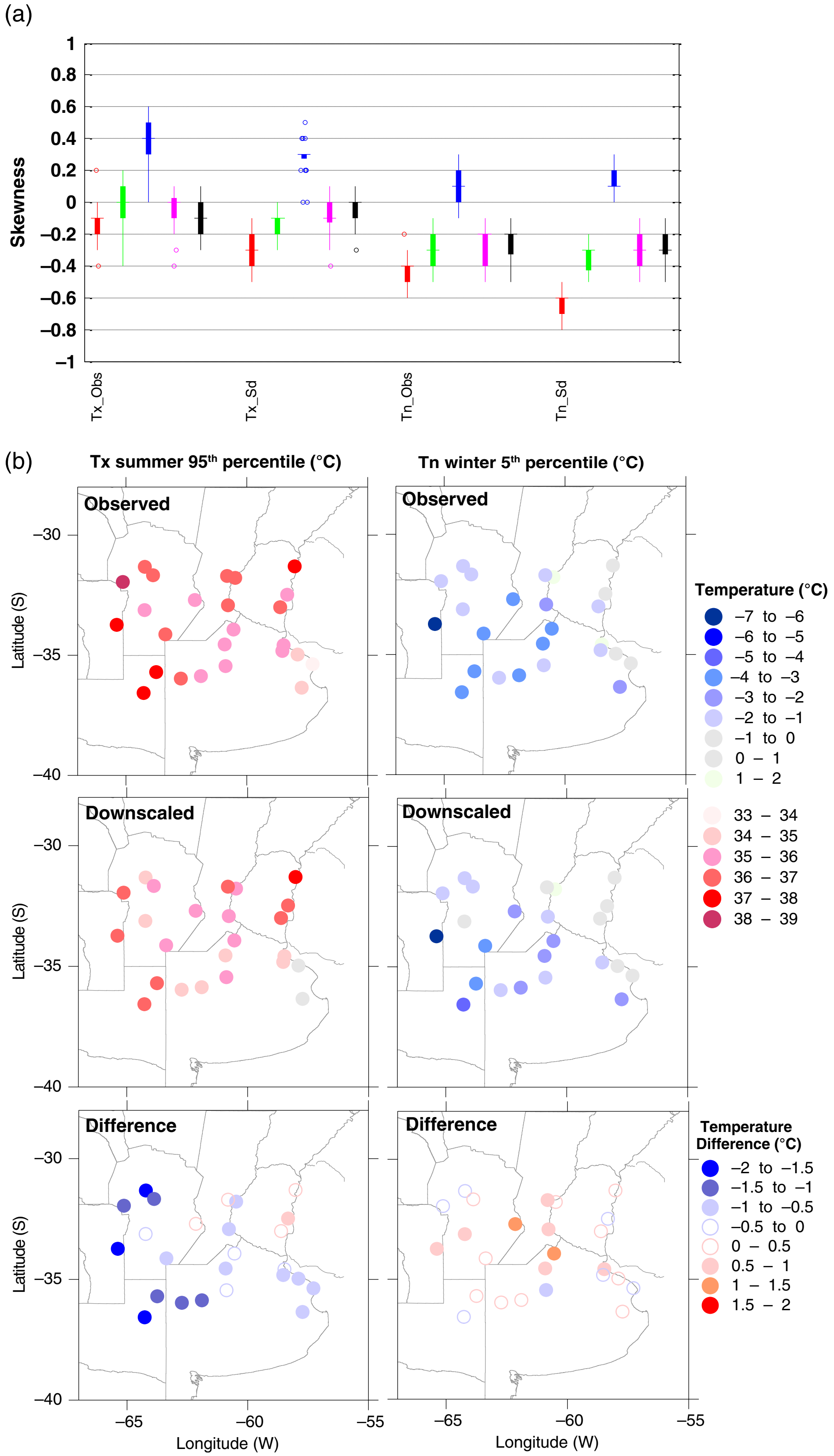

FIGURE 8 (a) Box and whisker plots of observed (Obs) and downscaled (Sd) skewness across all stations for Tx and Tn. Each group of five boxplots corresponds to summer (red), fall (green), winter (blue), spring (pink) and annual (black) periods. (b) Maps of observed and downscaled percentiles (°C) and differences (°C) between the downscaled and observed 95th percentile of maximum temperature in summer and 5th percentile of minimum temperature in winter [Colour figure can be viewed at wileyonlinelibrary.com]

significantly increased probability of occurrence of intense precipitation given a warm night (Tn90). This is a very important characteristic to be reproduced given that positive trends both in warm nights (Rusticucci and Barrucand, 2004) and in heavy rainfall events (Re and Barros, 2009; Penalba and Robledo, 2010) have been registered over part of the region and previous studies suggested that these increases are physically linked (Re and Barros, 2009).

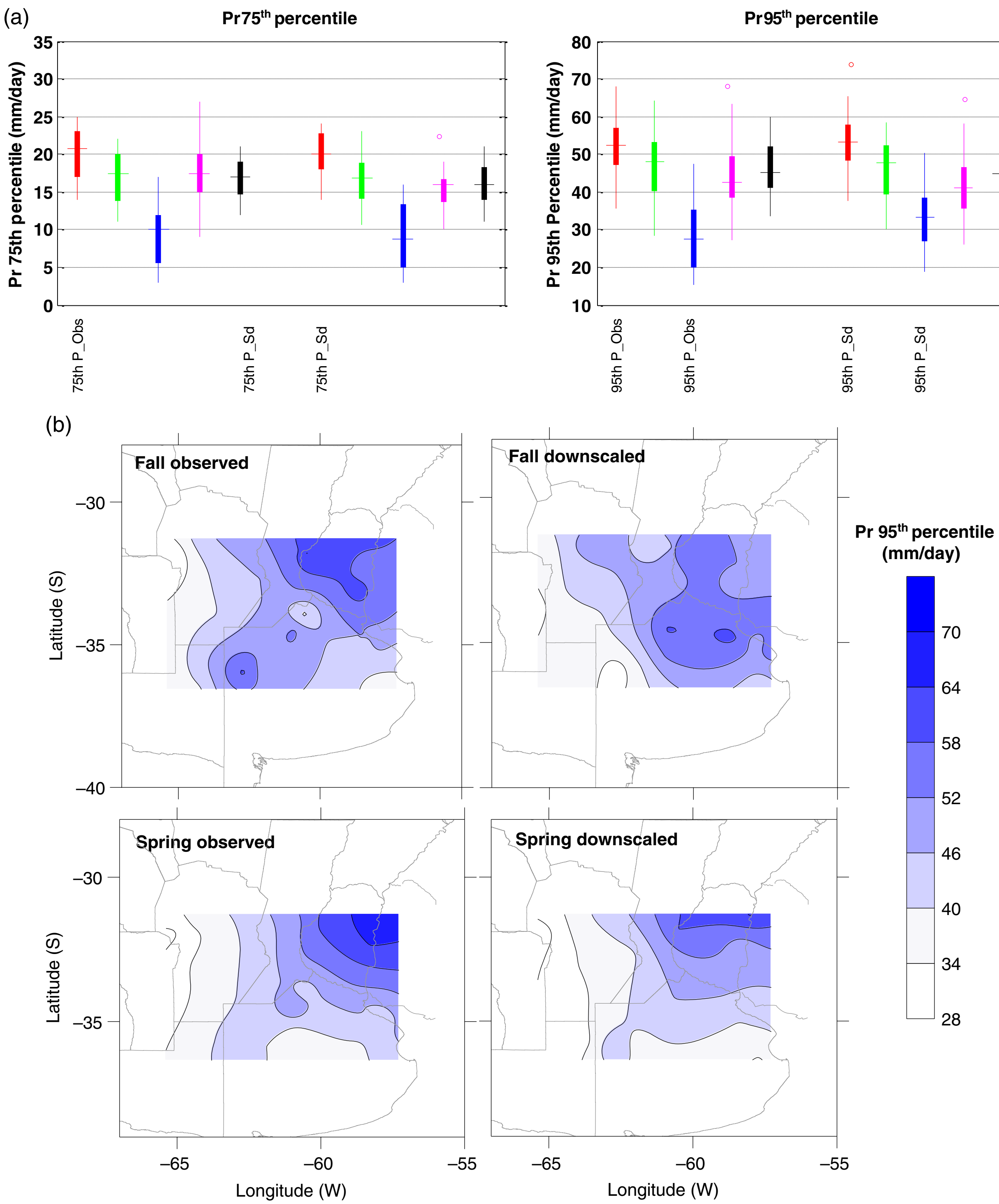

FIGURE 9 (a) Box and whisker plots of the observed (Obs) and downscaled (Sd) 75th and 95th percentile of wet days (mm/day) across all stations. Each group of five boxplots corresponds to summer (red), fall (green), winter (blue), spring (pink) and annual (black) periods. (b) Spatial distribution of the observed and downscaled 95th percentile of wet days (mm/day) during fall and spring. Note that isolines are plotted in order to better depict the spatial distribution [Colour figure can be viewed at wileyonlinelibrary.com]

On the other hand, Figure 11 shows how cold nights (Tn10) are associated with an inhibition of heavy precipitation. The ratios close to 0 indicate that the probability of occurrence of heavy precipitation events conditioned to extreme cold temperatures is low over the region. As suggested by Tencer *et al*. (2016) cold nights in the region are mainly related to anticyclones that lead to subsidence and weak surface winds together with low humidity and a clear sky, which is very well captured by the AN method. Although Figure 11 only shows the probabilities for summer and winter, this is observed in all the seasons of the year.

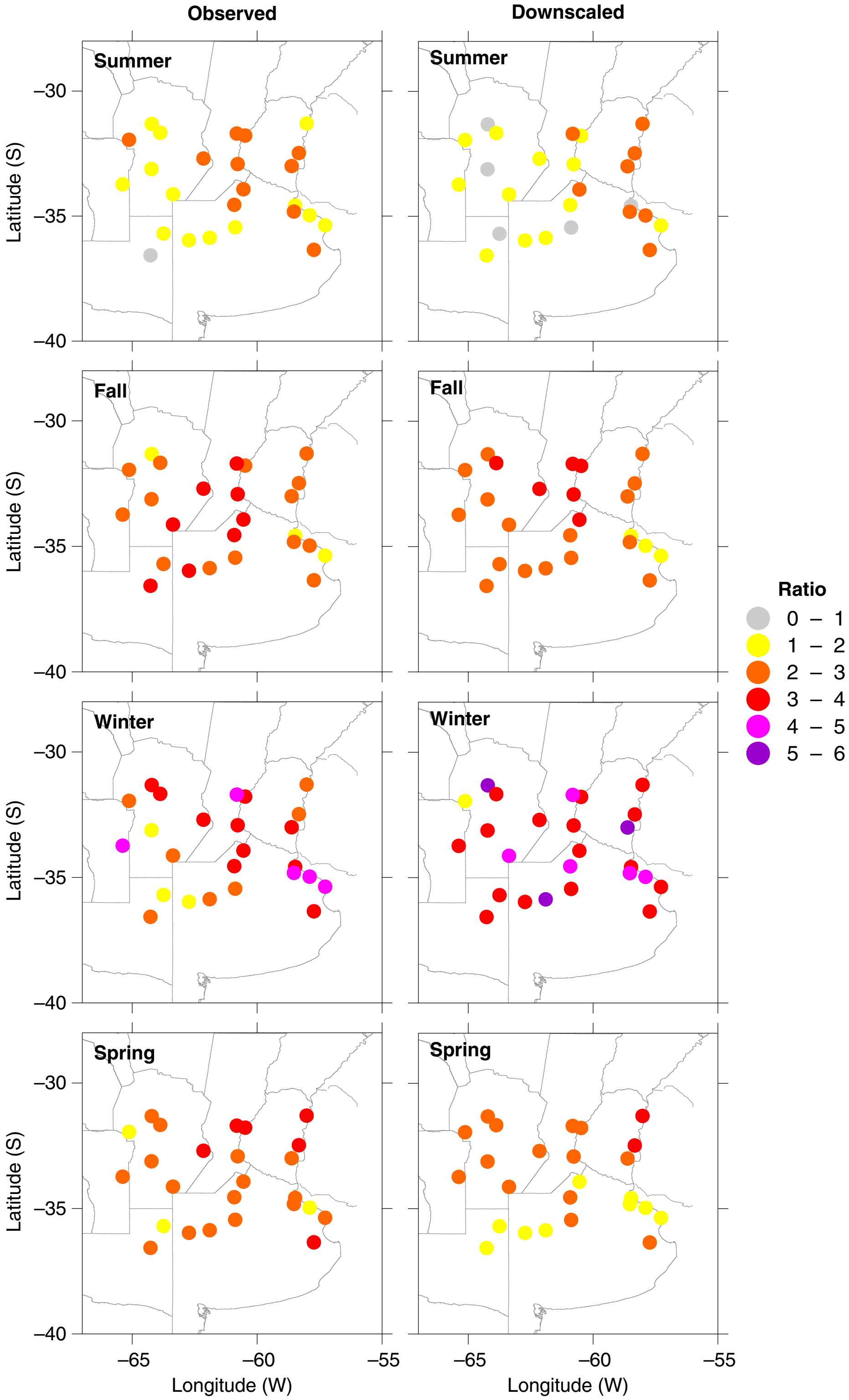

FIGURE 10 Observed and downscaled conditional probability of heavy precipitation events (days when precipitation exceeded the 75th percentile of the wet days) given the occurrence of a temperature extreme event (days when Tn exceeded the 90th percentile of the minimum temperature distribution) expressed as a ratio over the expected value in absence of statistical relationship during summer, fall, winter and spring [Colour figure can be viewed at wileyonlinelibrary.com]

4 | SUMMARY AND DISCUSSIONS

Given the extent of Argentina, its orography and the variety of its climate, it is expected that climate change affects differently in diverse regions of the country (Barros *et al.*, 2015). In this sense, it is of fundamental importance to provide climate information at a regional or local scale to design and implement mitigation and adaptation policies to climate change.

Among the approaches generally used for the generation of local or regional climate information, statistical downscaling methods are popular probably because of their low computational cost to be implemented. This characteristic makes them versatile and easy to apply to a large number of

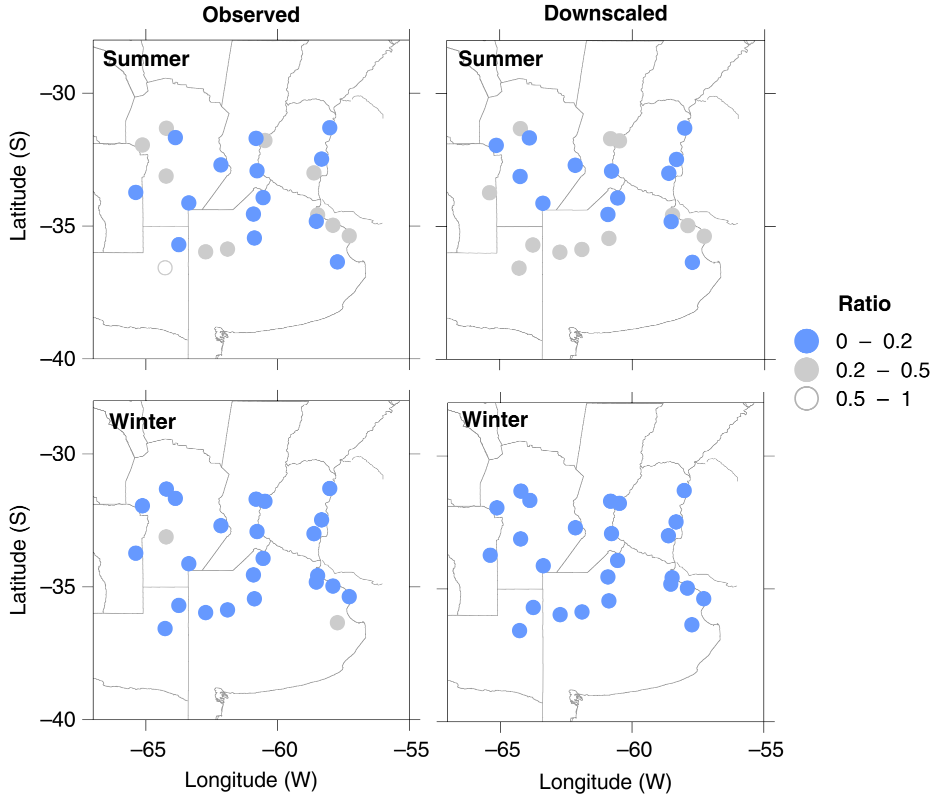

FIGURE 11 Observed and downscaled conditional probability of heavy precipitation events (days when precipitation exceeded the 75th percentile of the wet days) given the occurrence of a temperature extreme event (days when Tn is below the 10th percentile of the minimum temperature distribution) expressed as a ratio over the expected value in absence of statistical relationship during summer and winter [Colour figure can be viewed at wileyonlinelibrary.com]

GCMs for the generation of future projections of the regional climate and its associated uncertainty. However, ESD techniques have attributes and shortcomings that will depend, among other aspects, on the method itself, on the model construction or fitting and assumptions made, on the predictand variable and on the region of study. Therefore, it is important to carry out a comprehensive validation of the ESD methods, identifying their strengths and weaknesses, prior to the application in impact studies.

Despite the merits of the statistical downscaling methods, these techniques have not been validated or evaluated in southern South America as exhaustively as in other regions of the world. In this context, the objective of this work was to calibrate and validate the analogue method (AN) to downscale daily precipitation and temperatures in southern La Plata Basin. This region was particularly chosen due to its great socio-economic value and where there is increasing evidence of a changing climate with more frequent and more intense extreme events.

The statistical downscaling was carried out under the perfect prognosis approach (Maraun *et al.,* 2010). In this approach, statistical relationships are established based on observed large-scale predictors (in this case given by the reanalysis) and observed predictands (given by observed daily precipitation and maximum and minimum temperatures at station points). From this perspective, the selection of appropriate predictors constitutes a process of great importance because the performance of the ESD will depend, in part, on the choice of the predictor set. Taking into account that the predictors must be physically meaningful and realistically accurate, in this work different domains were tested considering the characteristics of the circulation in the south of South America. Special consideration was given to the effect of the Andes mountain range, which in the latitudes of the Pampas region reaches heights above 6,000 m. This large orographic barrier conditions circulation at low levels and may affect the performance of reanalysis.

Regarding the influence of the domain size for single predictors, it was observed that as the domain decreases, the performance of the ESD method does as well, stressing the importance of capturing the large-scale structures that control the regional climate. When combined predictors were considered, the ESD was found to be more skilful. For precipitation, this situation occurred when the humidity variables were incorporated into the predictor set. In this work, SLP in the middle domain, air temperature and specific humidity at 850 hPa were chosen as the predictor set for the subsequent analysis. However, it is important to underline that the degree of the method skill also depended on the predictor set, the season of year (though the model was built for the whole year) and the predictand variable. These aspects should be taken into account for the different applications, and in particular, when used in climate change studies, where predictors accounting for the radiation-induced changes are needed and the predictor–predictand relationship needs to be temporally stable.

Different aspects were evaluated in order to carry out a thorough assessment of the analogue method performance. The method showed an overall good performance. It tended to overestimate (underestimate) temperature values, especially during winter (summer), however the day-to-day variance during these seasons was fairly well represented. RMSE were smaller than the observed *SD* of Tx and Tn in all seasons of the year, stressing that the relative difference of the reconstructed and observed temperatures was smaller than their own variability. In all cases the analogue method improved the reproduction of the observed values when compared to direct reanalysis data, except for the daily correlations. The method showed some difficulties in representing the persistence, with autocorrelations lagged by 1 day slightly lower than observed. This characteristic is expected given that the AN method was built by searching the analogues independently for each day, therefore they did not keep the temporal evolution of large-scale atmospheric structures to preserve persistence. Distributional characteristics assessed by the two sample K-S test, extreme percentiles and skewness were adequately reproduced for minimum temperatures. For maximum temperatures, differences in probability distributions as a whole were detected. However, the AN method was able to reproduce extreme values and their spatial distributions for both temperatures despite its shortcoming of not being able to extrapolate outside of the observed range of values.

Modelling daily precipitation presents several challenges mainly related with its discontinuous nature in time and space. In this work, both precipitation occurrence and precipitation intensity were validated using different metrics. In general, the AN method performed well in reproducing different aspects of winter precipitation. The main reason for this may be that winter precipitation is mostly controlled by large-scale mechanisms that are well captured by the AN. However, some aspects such as wet day intensities, wet–wet and dry–wet transition probabilities, probability distributions and extremes were quite well represented during the warm season where local processes control precipitation. Spatial distributions of precipitation extremes characterized by the 95th percentile were also adequately reproduced in transition seasons. The method failed to reproduce the inter-annual variability of the seasonal precipitation amounts in all seasons of the year but it showed a better performance for the seasonal frequencies. Recent changes in summer precipitation seemed to be well captured by the method as it reproduced the increase (decline) in precipitation in stations located to the west (east) of the analysed domain. Although further analyses are needed regarding the stationarity assumption, which is a real limitation of ESD application under climate change conditions, these results increase confidence in the possibility of using this method in climate change studies. Similar conclusions were drawn by Timbal and Jones (2008), using the same technique though different predictors, for winter rainfall in southeast Australia.

The AN method tends, by construction, to reproduce the inter-variable dependence when the same predictor set is used for the three predictand variables. Therefore, the analysis was focused on compound extremes by assessing the reproduction of the conditional probability of heavy precipitation events given the occurrence of a minimum temperature extreme event (cold and warm) relative to the expected probability in the absence of a relationship. For both compound extremes, the intensity of the relationship as well as its spatial distribution was adequately reproduced by the AN method, except for the conditional probability of intense precipitation given high minimum temperatures in winter, where probabilities were slightly overestimated.

In general terms, the ESD method showed a very good potential for the generation of detailed climate information in the studied region. This makes it suitable for evaluation in different applications such as seasonal prediction or future projections under climate change scenarios. However, such applications are not without caveats that need to be investigated in future work, particularly the assessment of the time-invariance or stationarity assumption by considering, for instance, other calibration–validation approaches (Gutiérrez *et al.*, 2013) or climate model outputs as pseudo-observations (Vrac *et al.*, 2007; Gaitan *et al.*, 2014). Another aspect of great importance for the application of downscaling methods is an exhaustive evaluation of GCMs ability in representing the ESD predictors. Previous studies evaluated the performance of GCMs to represent daily SLP patterns in southern South America, finding an overall good representation (Penalba and Bettolli, 2011; Bettolli and Penalba, 2014). However, further validations are needed particularly for predictors such as air temperature or humidity variables. Overall, the results found in this work encourage us to continue exploring the advantages of the analogue method in producing local climate information for the different climatic regions in Argentina. In this line of work, different settings and implementations of the method could be subject for future research. These could include, among others, the use of the information of various nearest analogues (by considering the mean or a random selection of them), to test the sensitivity to the reanalysis choice or to use the extended EOF in the analogue search to consider the evolution of the large-scale structure that condition the local scale. Assessing the performance of different ESD methods apart from the analogue method would also be of great value in order to develop multi-method comparisons across the different regions of Argentina.

ACKNOWLEDGEMENTS

This work was supported by CONICET Grant PIP 0137 and UBA Grants 20020130100263BA and 200201302001 42BA.

ORCID

María Laura Bettolli http://orcid.org/0000-0001-7423-0544

REFERENCES

Agosta, E.A. and Compagnucci, R.H. (2012) Central-West Argentina summer precipitation variability and atmospheric teleconnections. *Journal of Climate*, 25, 1657–1677.

de Barros Soares, D., Lee, H., Loikith, P.C., Barkhordariana, A. and Mechoso, C.R. (2016) Can significant trends be detected in surface air temperature and precipitation over South America in recent decades? *International Journal of Climatology*, 37, 1483–1493. https://doi.org/10.1002/joc.4792.

Barros, V.R., Doyle, M., González, M., Camilloni, I., Bejarán, R. and Caffera, R.M. (2002a) Climate variability over subtropical South America and the South American monsoon: a review. *Meteorologica*, 27, 33–57.

Barros, V.R., Grimm, A. and Doyle, M.E. (2002b) Relationship between temperature and circulation in southeastern South America and its influence from El Niño and La Niña events. *Journal of the Meteorological Society of Japan*, 80, 21–32.

Barros, V.R., Clarke, R. and Silva, D.P. (2006) Climate change in the La Plata Basin. In: *La Plata Basin Climatology*, 1st edition. Buenos Aires: Consejo Nacional de Investigaciones Científicas y Técnicas (CONICET).

Barros, V.R., Boninsegna, J.A., Camilloni, I.A., Chidiak, M., Magrín, G.O. and Rusticucci, M.M. (2015) Climate change in Argentina: trends, projections, impacts and adaptation. *WIREs Climate Change*, 6, 151–169. https://doi.org/10.1002/wcc.316.

Benestad, R.E. (2010) Downscaling precipitation extremes: correction of analog models through PDF predictions. *Theoretical and Applied Climatology*, 100, 1–21. https://doi.org/10.1007/s00704-009-0158-1.

Benestad, R.E., Hanssen-Baur, I. and Chen, D. (2008) *Empirical-statistical Downscaling*. Singapore: World Scientific.

Bettolli, M.L. and Penalba, O.C. (2014) Synoptic sea level pressure patterns-daily rainfall relationship over the Argentine Pampas in a multi-model simulation. *Meteorological Applications*, 21, 376–383.

Bettolli, M.L., Altamirano del Carmen, M.A., Cruz Brasesco, G., de MoraesRudorff, F., Martinez Ortiz, A., Armoa Cañete, J. and Arroyo, J. (2010a) Natural pasture in Salto (Uruguay): relationship with climate variability and analysis in the context of future climate change. *Revista Brasileira de Meteorologia*, 25, 248–259.

Bettolli, M.L., Penalba, O.C. and Vargas, W.M. (2010b) Synoptic weather types in the south of South America and their relationship to daily rainfall in the core production region of crops in Argentina. *Australian Meteorological and Oceanographic Journal*, 60, 37–48.

Brands, S., Taboada, J.J., Cofiño, A.S., Sauter, T. and Schneider, C. (2011) Statistical downscaling of daily temperatures in the NW Iberian Peninsula from global climate models: validation and future scenarios. *Climate Research*, 48, 163–176. https://doi.org/10.3354/cr00906.

Cavazos, T. and Hewitson, B.C. (2005) Performance of NCEP-NCAR reanalysis variables in statistical downscaling of daily precipitation. *Climate Research*, 28, 95–107.

D'onofrio, A., Boulanger, J.P. and Segura, E.C. (2010) CHAC: a weather pattern classification system for regional climate downscaling of daily precipitation. *Climatic Change*, 98, 405–427.

Espinoza, J.C., Ronchail, J., Lengaigne, M., Quispe, N., Silva, Y., Bettolli, M. L., Avalos, G. and Llacza, A. (2012) Revisiting wintertime cold air intrusions at the east of the Andes: propagating features from subtropical Argentina to Peruvian Amazon and relationship with large-scale circulation patterns. *Climate Dynamics*, 41, 1983–2002.

Frost, A.J., Charles, S.P., Timbal, B., Chiew, F.H.S., Mehrotra, R., Nguyen, K. C., Chandler, R.E., McGregor, J.L., Fu, G., Kirono, D.G.C., Fernandez, E. and Kent, D.M. (2011) A comparison of multi-site daily rainfall downscaling techniques under Australian conditions. *Journal of Hydrology*, 408, 1–18.

Gaitan, C.F., Hsieh, W.W. and Cannon, A.J. (2014) Comparison of statistically downscaled precipitation in terms of future climate indices and daily variability for southern Ontario and Quebec, Canada. *Climte Dynamics*, 43, 3201–3217. https://doi.org/10.1007/s00382-014-2098-4.

Giorgi, F. and Mearns, L.O. (1991) Approaches to the simulation of regional climate change: a review. *Reviews of Geophysics*, 29, 191–216.

Goodess, C. (2005) *STARDEX, downscaling climate events*. Norwich: University of East Anglia. Available at: https://crudata.uea.ac.uk/projects/stardex/-reports/STARDEX_FINAL_REPORT.pdf.

Gutiérrez, J.M., Cano, R., Cofiño, A.S. and Sordo, C. (2005) Analysis and downscaling multi-model seasonal forecasts in Peru using self-organizing maps. *Tellus A*, 57, 435–447.

Gutiérrez, J.M., San Martín, D., Brands, S., Manzanas, R. and Herrera, S. (2013) Reassessing statistical downscaling techniques for their robust application under climate change conditions. *Journal of Climate*, 26, 171–188. https://doi.org/10.1175/JCLI-D-11-00687.1.

Haylock, M.R., Cawley, G.C., Harpham, C., Wilby, R.L. and Goodess, C.M. (2006) Downscaling heavy precipitation over the United Kingdom: a comparison of dynamical and statistical methods and their future scenarios. *International Journal of Climatology*, 26, 1397–1415. https://doi.org/10.1002/joc.1318.

Hewitson, B.C. and Crane, R.G. (1996) Climate downscaling techniques and applications. *Climate Research*, 7, 85–95.

Hewitson, B.C. and Crane, R.G. (2006) Consensus between GCM climate change projections with empirical downscaling: precipitation downscaling over South Africa. *International Journal of Climatology*, 26, 1315–1337.

Huth, R. (1999) Statistical downscaling in central Europe: evaluation of methods and potential predictors. *Climate Research*, 13, 91–101.

Huth, R. (2004) Sensitivity of local daily temperature change estimates to the selection of downscaling models and predictors. *Journal of Climate*, 17, 640–652.

Huth, R., Mikšovský, J., Štěpánek, P., Belda, M., Farda, A., Chládová, Z. and Pišoft, P. (2015) Comparative validation of statistical and dynamical downscaling models on a dense grid in central Europe: temperature. *Theoretical and Applied Climatology*, 120, 533–553. https://doi.org/10.1007/s00704-014-1190-3.

Imbert, A. and Benestad, R.E. (2005) An improvement of analog model strategy for more reliable local climate change scenarios. *Theoretical and Applied Climatology*, 82, 245–255.

INDEC. (2010) *National Institute of Statistics and Censuses (INDEC), census 2010*. Available at: https://www.indec.gov.ar/el-indec-eng.asp.

Kanamitsu, M., Ebisuzaki, W., Woollen, J., Yang, S.-K., Hnilo, J.J., Fiorino, M. and Potter, G.L. (2002) NCEP-DOE AMIP-II reanalysis (R-2). *Bulletin of the American Meteorological Society*, 83, 1631–1643.

Labraga, J.C. (2010) Statistical downscaling estimation of recent rainfall trends in the eastern slope of the Andes mountain range in Argentina. *Theoretical and Applied Climatology*, 99, 287–302.

Maenza, R., AgostaScarel, E.A. and Bettolli, M.L. (2017) Climate change and precipitation variability over the western "Pampas" in Argentina. *International Journal of Climatology*, 37, 445–463. https://doi.org/10.1002/joc.5014.

Maraun, D., Wetterhall, F., Ireson, A.M., Chandler, R.E., Kendon, E.J., Widmann, M., Brienen, S., Rust, H.W., Sauter, T., Themeßl, M., Venema, V.K.C., Chun, K.P., Goodess, C.M., Jones, R.G., Onof, C., Vrac, M. and Thiele-Eich, I. (2010) Precipitation downscaling under climate change. Recent developments to bridge the gap between dynamical models and the end user. *Reviews of Geophysics*, 48, 1–34.

Maraun, D., Widmann, M., Gutiérrez, J.M., Kotlarski, S., Chandler, R.E., Hertig, E., Wibig, J., Huth, R. and Wilcke, R.A.I. (2015) VALUE: a framework to validate downscaling approaches for climate change studies. *Earth's Future*, 3, 1–14. https://doi.org/10.1002/2014EF000259.

Maraun, D., Huth, R., Gutiérrez, J.M., San Martín, D., Dubrovsky, M., Fischer, A., Hertig, E., Soares, P.M.M., Bartholy, J., Pongrácz, R., Widmann, M., Casado, M.J., Ramos, P. and Bediae, J. (2017) The VALUE perfect predictor experiment: evaluation of temporal variability. *International Journal of Climatology*. https://doi.org/10.1002/joc.5222.

Meehl, G.A., Covey, C., Delworth, T.L., Latif, M., McAveney, B., Mitchell, J. F.B., Stouffer, R.J. and Taylor, K.E. (2007) The WCRP CMIP3 multimodel dataset: a new era in climate change research. *Bulletin of the American Meteorological Society*, 88, 1383–1394. https://doi.org/10.1175/BAMS-88-9-1383.

Menéndez, C.G., de Castro, M., Boulanger, J.-P., D'Onofrio, A., Sanchez, E., Sörensson, A.A., Blazquez, J., Elizalde, A., Jacob, D., Le Treut, H., Li, Z. X., Núñez, M.N., Pessacg, N., Pfeiffer, S., Rojas, M., Rolla, A., Samuelsson, P., Solman, S.A. and Teichmann, C. (2009) Downscaling extreme month-long anomalies in southern South America. *Climatic Change*, 98, 379–403. https://doi.org/10.1007/s10584-009-9739-3.

Penalba, O.C. and Bettolli, M.L. (2011) Climate change impacts on atmospheric circulation and daily precipitation in the Argentine Pampas region. In: Blanco, J. (Ed.) *Climate Change: Geophysical Foundations and Ecological Effects*. Rijeka: InTech, ISBN: 978-953-307-419-1.

Penalba, O.C. and Robledo, F.A. (2010) Spatial and temporal variability of the frequency of extreme daily rainfall regime in the La Plata Basin during the 20th century. *Climatic Change*, 98, 531–550.

Penalba, O.C. and Vargas, W.M. (2004) Interdecadal and interannual variations of annual and extreme precipitation over central-northeastern Argentina. Changes in the extreme precipitation seasonal cycle. *International Journal of Climatology*, 24, 1565–1580.

Penalba, O.C., Bettolli, M.L. and Krieger, P.A. (2013) Surface circulation types and daily maximum and minimum temperatures in southern La Plata Basin. *Journal of Applied Meteorology and Climatology*, 52, 2450–2459.

Re, M. and Barros, V.R. (2009) Extreme rainfalls in SE South America. *Climatic Change*, 96, 119–136.

Ribalaygua, J., Torres, L., Pórtoles, J., Monjo, R., Gaitán, E. and Pino, M.R. (2013) Description and validation of a two-step analogue/regression downscaling method. *Theoretical and Applied Climatology.*, 114, 253–269. https://doi.org/10.1007/s00704-013-0836-x.

Robledo, F.A., Penalba, O.C. and Bettolli, M.L. (2013) Teleconnections between tropical–extratropical oceans and the daily intensity of extreme rainfall over Argentina. *International Journal of Climatology*, 33, 735–745.

Rummukainen, M. (2010) State-of-the-art with regional climate models. *WIREs Climate Change*, 1, 82–96. https://doi.org/10.1002/wcc.8.

Rusticucci, M. (2012) Observed and simulated variability of extreme temperature events over South America. *Atmospheric Research*, 106, 1–17.

Rusticucci, M. and Barrucand, M.G. (2001) Extreme temperatures over Argentina. Quality control. Association between extreme daily temperature frequency and seasonal mean. *Meteorologica*, 26, 69–83.

Rusticucci, M. and Barrucand, M. (2004) Observed trends and changes in temperature extremes over Argentina. *Journal of Climate*, 17, 4099–4107.

Saurral, R.I., Camilloni, I.A. and Barros, V.R. (2017) Low-frequency variability and trends in centennial precipitation stations in southern South America. *International Journal of Climatology*, 37, 1774–1793. https://doi.org/10.1002/joc.4810.

Schmidli, J., Goodess, C.M., Frei, C., Haylock, M.R., Hundecha, Y., Ribalaygua, J. and Schmith, T. (2007) Statistical and dynamical downscaling of precipitation: an evaluation and comparison of scenarios for the European Alps. *Journal of Geophysical Research*, 112, D04105. https://doi.org/10.1029/2005JD007026.

Schoof, J. and Pryor, S. (2001) Downscaling temperature and precipitation: a comparison of regression-based methods and artificial neural networks. *International Journal of Climatology*, 21, 773–790.

Seluchi, M.E. and Marengo, J.A. (2000) Tropical–midlatitude exchange of air masses during summer and winter in South America: climatic aspects and examples of intense events. *International Journal of Climatology*, 20, 1167–1190.

Silvestri, G. and Vera, C. (2008) Evaluation of the WCRP-CMIP3 model simulations in the La Plata Basin. *Meteorological Applications*, 15, 497–502. https://doi.org/10.1002/met.98.

Solman, S. and Núñez, M. (1999) Local estimates of global change: a statistical downscaling approach. *International Journal of Climatology*, 19, 835–861.

Tencer, B., Bettolli, M.L. and Rusitcucci, M. (2016) Compound temperature and precipitation extreme events in southern South America: associated atmospheric circulation and simulations by a multi-RCM ensemble. *Climate Research*, 68, 183–199. https://doi.org/10.3354/cr01396.

Timbal, B. (2004) Southwest Australia past and future rainfall trends. *Climate Research*, 26, 233–249.

Timbal, B. and Jones, D.A. (2008) Future projections of winter rainfall in southeast Australia using a statistical downscaling technique. *Climatic Change*, 86, 165–187.

Timbal, B. and McAvaney, B.J. (2001) An analogue-based method to downscale surface air temperature: application for Australia. *Climate Dynamics*, 17, 947–963.

Timbal, B., Dufour, A. and McAvaney, B. (2003) An estimate of future climate change for western France using a statistical downscaling technique. *Climate Dynamics*, 20, 807–823.

Vrac, M., Stein, M.L., Hayhoe, K. and Liang, X.-Z. (2007) A general method for validating statistical downscaling methods under future climate change. *Geophysical Research Letters*, 34, L18701. https://doi.org/10.1029/2007GL030295.

Wilby, R.L. and Wigley, T.M.L. (1997) Downscaling general circulation model output: a review of methods and limitations. *Progress in Physical Geography*, 21, 530–548.

Wilby, R.L., Dawson, C.W. and Barrow, E.M. (2002) SDSM—a decision support tool for the assessment of regional climate change impacts. *Environmental Modelling and Software*, 17, 147–159.

Wilby, R.L., Charles, S.P., Zorita, E., Timbal, B., Whetton, P. and Mearns, L.O. (2004) Guidelines for use of climate scenarios developed from statistical downscaling methods. In: *IPCC Task Group on Data and Scenario Support for Impact and Climate Analysis (TGICA) Geneva, Switzerland.* Available at: http://www.ipcc-data.org/guidelines/index.html.

Wilks, D.S. (2006) *Statistical Methods in the Atmospheric Sciences*. San Diego, CA: Academic Press.

Zorita, E. and von Storch, H. (1999) The analog method as a simple statistical downscaling technique: comparison with more complicated methods. *Journal of Climate*, 12, 2474–2489.

How to cite this article: Bettolli ML, Penalba OC. Statistical downscaling of daily precipitation and temperatures in southern La Plata Basin. *Int J Climatol*. 2018;38:3705–3722. https://doi.org/10.1002/joc.5531